

Exact electron states in $1D$ (quasi-) periodic arrays of delta-potentials.

Peter Kramer and Tobias Kramer
Institut für Theoretische Physik der Universität
Tübingen, Germany.

25th October 2018

1 Introduction and Scope.

In the solid state physics of crystals, an important part is played by the band structure of the electronic states. This band structure arises from the representation of the periodicity in the electronic state space. Powerful computational methods were developed for the calculation of band structures, among them the linear muffin-tin (LMTO) method [17] in the atomic sphere approximation (ASA) [1]. In the physics of quasicrystals, it is believed that the electronic system plays an important part [19]. Here one is lacking the periodic symmetry. To still use the powerful methods of band computations, one must replace the quasicrystal by a periodic approximant. The question arises how such approximant computations approach a quasiperiodic limit. In a recent calculation [6] it is shown by a supercell analysis that an approximant computation may lead to artefacts in the electronic density of states (DOS). More detailed local properties of the electrons appear as derivatives of the electronic charge density in Mössbauer studies on quasicrystals [14].

In the present work we wish to analyse and compare electronic states in periodic and quasiperiodic potentials in a way free of approximations. In this way we can hope to address the similarities and differences of these systems from first principles.

To a first and very important approximation, the many-electron states in ordered crystalline or quasicrystalline solids are constructed from one-electron states, compare for example Ashcroft and Mermin [2], after appropriate antisymmetrization. The one-electron Hamiltonian then contains periodic and quasiperiodic potentials respectively. For a general account of band theory

we refer to Blount [4]. Analytic properties and the approach due to Wannier [20] are discussed by Kohn [8]. For general electronic structures beyond periodicity, a local view was advocated by Heine [7] who proposed to throw out K -space.

In what follows we wish to elaborate and to compare electronic systems and their local structure in terms of the following concepts:

(i) Local view of K -space in periodic potentials:

A Hamiltonian with an infinite *periodic potential* has the discrete symmetry group Λ of its lattice. The electron states are characterized by the irreducible representations of Λ . These are labelled by the continuous set of Bloch vectors K from the Brillouin zone, that is, the first unit cell of the reciprocal lattice Λ^R . The eigenstates for fixed energy $E(K)$ are the Bloch states belonging to the bands.

A local formulation of K -space arises as follows: Wigner and Seitz [21] in 1934 introduced the *cellular method*: The one-electron Schrödinger equation with fixed energy E is to be solved exclusively on the finite unit cell of the lattice with the *local boundary conditions* that the solution, after propagation over a full primitive period say a_j , $j = 1, 2, 3$, picks up a pure phase factor. This phase factor when written in the form $f_j := \exp(iK_j a_j)$, $j = 1, 2, 3$ determines the Bloch labels. Two solutions with $K \rightarrow -K$ are degenerate. The energy $E(K)$ appears in bands, with Bloch labels ranging over the Brillouin zone, and in gaps where there are no states with Bloch type boundary conditions. This approach allows an extension to finite and to infinite systems. Within bands, the solutions can be matched and propagated as Bloch states over all the cells of the crystal.

(ii) Local view of K -space in quasiperiodic potentials:

For infinite almost periodic systems in $1D$ some general results with many references are discussed in [5]. For another detailed study of discrete systems with many references we quote Sütö [18]. For our purposes we consider an infinite *quasiperiodic potential* built from a few basic cells as in a tiling model for quasicrystals. For each cell one can apply the local analysis of Wigner and Seitz with local Bloch type boundary conditions. Quasiperiodicity now requires a matching of these local boundary conditions between the basic cells. It is not enough that, at fixed energy E , each cell separately admits Bloch type boundary conditions. We must also check if a patch of cells admits these boundary conditions. Again one can study the quasiperiodic extension of the system, following for example a geometric inflation of the tiling.

(iii) Local view, positive and negative energy, motive clusters:

Imagine the atomic nuclei of a unit cell in a periodic crystal to form a free

motive cluster. This motive cluster is not unique since the unit cell of a crystal admits translations as well as transformation of shape, for example in going from the primitive to the Wigner-Seitz cell.

For a fixed choice of motive clusters we should not relax the positions of the nuclei to gain energy, as would be done in real molecules, since in the crystal the positions are controlled by *all* atomic neighbours.

Example: Take for example a linear crystal with two atoms A, B , in two spacings $a \neq b$ with the sequence $AaBbAaBbAa\dots$ and period $a + b$. Choose two different motive clusters by the replacements $AaBb \rightarrow AaB$ and $BbAa \rightarrow BbA$ which do not affect the bound states. We get in general two different bound states, with the binding energy depending on the relative distances a and b respectively. In a linear molecule we would relax the distance and end up in both cases at the same binding energy. This is not allowed in the crystal! In the linear crystal *the two different motive clusters generate identical periodic structures and bands!*

Consider then the one-electron bound states for the chosen motive cluster. It is true that, in order to treat it like a molecule, we should take along the nuclei and their Coulomb repulsion. However since we keep the nuclei at fixed positions we may neglect these interactions which of course influence the binding and the total energy. Independent of these interaction terms, the different boundary conditions of the electron states at positive or negative energy will enter into the computation of the many-electron states.

Since the Hamiltonian for fixed nuclear positions is the same as in the Wigner-Seitz method, the only difference is in the boundary conditions which for a bound state require the solutions to decay exponentially. Clearly now we must distinguish between the *positive and negative energy region*. The former admits scattering states, the latter bound states.

The infinite systems at positive energy should here be considered as an approximation to a finite macroscopic systems which still admits a scattering experiment. We could also consider half-infinite systems which allow at least for backscattering. For both finite and infinite systems, the distinction between positive and negative energy states is crucial. In considering finite patches of periodic or quasiperiodic systems one therefore should pay attention to the sign of the energy.

(iv) **Bound, Bloch and scattering states in periodic potentials:**

We shall term the negative energy region the *exact tight binding scenario* in what follows. As a partial differential equation of second order, the stationary Schrödinger equation has two fundamental solutions on a single cell. Suppose that the energy of a bound state lies within the range of energy for a band. Then it follows from the Schrödinger equation that *the bound state solution*

restricted to the unit cell must be an exact linear combination of the local Bloch states at the bound state energy. In the positive energy region we can still obtain states with local Bloch boundary conditions. Now we can inquire how the band structure of these positive energy states is related to one-electron scattering states.

Example: The relation of bound and Bloch states in crystals is often considered in approximate rather than exact computations, as for example in the *tight binding approximation*. Here one starts exclusively from bound atomic l-orbitals of the isolated atoms, obtains the Bloch states from their tunneling to next neighbours, and labels the bands by the l-orbitals. If first-order degenerate perturbation theory applies, the energies in the bands result from the splitting of the single orbital whose degeneracy is proportional to the number of atoms. In this approximation it is clear that the energy of the local atomic orbital is within the corresponding band. In many cases the bound atomic orbitals of the atoms in the cell are separated in energy. Otherwise one can consider hybrid or motive cluster orbitals on the unit cell as the origin of band labels. The discrete version of this approximation leads to an eigenvalue problem and therefore loses the information on the sign of the energy.

The general arguments given above are valid *independent of any such approximation scheme*. They show that *in the exact tight binding scenario there must exist an exact local relation between bound and Bloch states*.

(v) Bound, Bloch and scattering states in quasiperiodic potentials: For a quasiperiodic potential based on a tiling, we again wish to distinguish the negative and positive energy regions. One can consider at negative energy the bound states for finite patches which form part of a quasiperiodic structure and compare with states obeying local Bloch type boundary conditions on the same patch. We refer to such an energy range as a *band germ* and to the local Bloch states as *Bloch germs*. If the bound state energy admits Bloch type boundary conditions, it must be possible to express the bound states by pairs of local Bloch states (germs). The bound states may be related to local clusters.

In the scattering from quasiperiodic potentials at positive energy, the aim is again to compute the scattering matrix. For an exact computation one may inquire about the implication of inflation symmetry on the scattering matrix.

In what follows we wish to demonstrate the validity of these concepts in a way free of approximations. In dimension three we cannot yet implement exact examples for these concepts. The LMTO method may allow to examine some of our points. We choose here a comparative and specific study

restricted to continuous periodic and quasiperiodic potentials in dimension one. On them we wish to demonstrate the concepts given above by exact computations. To do so we pay the price of choosing simple delta potentials even of the same strength. We explore the electron states in terms of local boundary conditions, in the spirit of the Wigner-Seitz approach, applied to finite strings (patches) which form part of periodic or quasiperiodic structures. We shall always start from finite patches and then look into their recursive extension. The solutions with Bloch boundary conditions on a finite string are systematically compared with bound state solutions on the same string. The main tool of our analysis is the continuous transfer matrix which is well defined for piecewise constant potentials, including delta potentials as a limiting case. This matrix propagates by matrix multiplication a fundamental system of two solutions. We shall stress in what follows the polynomial dependence of the matrix elements on the strength parameter of the delta potential. This will allow us to order and analyze the matrix systems.

2 Finite periodic strings at negative energy.

2.1 Preview: An energy gauge for crystals.

As an introduction we present some material from [12]. We rephrase the well-known periodic case [15]. Consider first a finite string S with the transfer matrix M , described in more detail in section 2.2. We define an *energy gauge* f as a function with value $f = 0$ on an energy interval such that $|\text{tr}(M)| \leq 1$ and $f = 1$ otherwise, compare Fig. 1. We call this a *band germ*. The condition on the trace assures that inside the band germ M has two complex conjugate eigenvalues of absolute value 1. Repeat the string n times to produce a new transfer matrix M^n . Since the existence of band germs is related to the eigenvalue problem, the range of energies for which $\frac{1}{2}|\text{tr}(M^n)| < 1$ is *independent of n , the band germs stay the same on the new string*. The Bloch germs propagate through the string and pick up the same phase factors respectively after each transmission.

Consider next the bound states of the string M^n . In a very tight binding case we claim

1 Prop: The bound states of the string M^n may be grouped into sets of n states, where the energies of each such set corresponds to a part $f = 0$ of the energy gauge f of the string M .

Proof: For very tight binding it suffices to use first-order degenerate perturbation theory, applied to the bound states of the single atoms: To this order, the bound states of the string are the eigenvalues of a matrix whose

off-diagonal entries are the weak atom-atom cross terms. By standard matrix theory, the maximum level splitting will increase with n . But band theory tells us that in the limit $n \rightarrow \infty$ all energies stay inside the band, hence inside the initial band germ. Thus the energy of all these bound states for finite n must stay within the energy gauge of the (single) band germ.

We now have the following situation in the finite string M^n : In a band germ from the string M , there is for each energy value a pair of Bloch germs which can carry charge current. There are now n discrete bound states with the energy gauge as in the initial string.

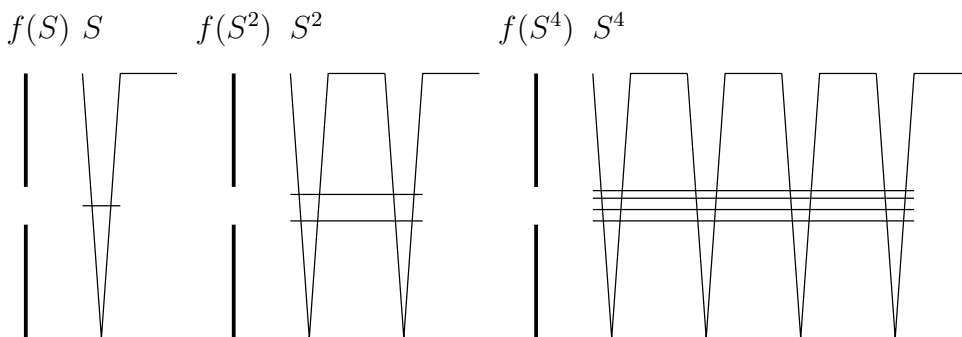


Fig.1: Periodic strings: The string S to the left has one attractive δ -well with a single bound state, followed by a tunnel. The vertical bar to its left shows the energy interval for the band germ. This interval is the energy gauge $f(S)$ comprising the bound state. The string S^2 in the middle has two attractive δ -potentials and two bound states. The energy gauge $f(S^2)$ is unchanged but comprises two bound states. The same energy gauge $f(S^4)$ for the string S^4 to the right comprises four bound states.

A schematic view of the periodic scheme is given in Fig.1. Now we can extend the analysis to $n \rightarrow \infty$:

2 Prop: For an infinite periodic repetition of a fixed string, the energy gauge stays the same as for the initial string. The band germ generates a band. Within each band there is an *infinite set of (pairs of) Bloch states whose energies $E_K < 0$ fill up the original band germ.*

2.2 Bloch and bound states in a single band.

We shall use the notation of [10]. Consider the 1D Schrödinger stationary equation on the line $x \in \mathbf{R}$,

$$\left[-\frac{\hbar^2}{2m} \frac{d^2}{dx^2} + V(x) \right] \phi(x) = E\phi(x). \quad (1)$$

with $V(x)$ a piecewise constant potential. Denote two fundamental solutions and their derivatives by $\phi_1(x), \phi_1'(x), \phi_2(x), \phi_2'(x)$. Choose the initial values $\phi_1(0) = 1, \phi_1'(0) = 0, \phi_2(0) = 0, \phi_2'(0) = 1$ which implies a Wronskian equal to 1. The 2×2 standard transfer matrix is defined as

$$\begin{aligned} M(x) &= \begin{bmatrix} \phi_1(x) & \phi_2(x) \\ \phi_1'(x) & \phi_2'(x) \end{bmatrix}, \\ M(0) &= 1. \end{aligned} \tag{2}$$

The transfer matrix obeys the first-order system of equations which is equivalent to the Schrödinger equation. A *second interpretation* of the transfer matrix, which we shall adopt in what follows, results because the matrix $M(x)$ can also be shown to *propagate the fundamental system*.

The Schrödinger equation for piecewise constant potentials on a finite string can now be solved as follows [12]: We first determine the transfer matrix for simple building blocks of finite size at the fixed energy. Then we propagate the solutions over the full string by matrix multiplication. This matrix multiplication guarantees the continuity of the solutions and of their derivatives. Specific boundary conditions can finally be met by determining the appropriate linear combination of the two fundamental solutions. For real matrices with Wronski determinant 1 the transfer matrices belong to the matrix group $SL(2, R)$. More details on this group and the isomorphic group $SU(1, 1)$ can be found in [10]. One should be careful in applying the group concepts to the transfer matrices, as can be seen from the following transformation properties.

It will prove convenient to pass to a new fundamental systems of solutions by choosing different initial values. With respect to the matrix formed by the solutions, this transformation is achieved by *right multiplication with a constant matrix*,

$$M(x) \rightarrow M(x)C \tag{3}$$

The *new transfer matrix which propagates the new system* $M(x)C$ is no longer equal to $M(x)C$, instead it *is given by* $C^{-1}M(x)C$. This propagating transfer matrix by itself does not admit an interpretation in terms of fundamental solutions and their derivatives!

We now pass to a new system of fundamental solutions with different initial conditions by right multiplication with the matrix

$$\tilde{R} := \sqrt{i} R = \sqrt{\frac{1}{2\kappa}} \begin{bmatrix} 1 & 1 \\ -\kappa & \kappa \end{bmatrix}. \tag{4}$$

The system corresponding to the matrix $M(x)\tilde{R}$ has the initial data \tilde{R} at $x = 0$. At negative energy $E = -\frac{\hbar^2}{2m}\kappa^2$ we define a *tunnel* as a string with

vanishing potential. In a tunnel the transfer matrix takes the form

$$M(x)\tilde{R} = \sqrt{\frac{1}{2\kappa}} \begin{bmatrix} \exp(-\kappa x) & \exp(\kappa x) \\ -\kappa \exp(-\kappa x) & \kappa \exp(\kappa x) \end{bmatrix}. \quad (5)$$

The transfer matrix which propagates this new system at negative energy is given by

$$\begin{aligned} \tilde{M}(x) &:= \tilde{R}^{-1}M(x)\tilde{R} \\ &= \begin{bmatrix} \exp(-\kappa x) & 0 \\ 0 & \exp(\kappa x) \end{bmatrix} \end{aligned} \quad (6)$$

For a bound state we require that an exponentially increasing function at negative energy on the left-hand tunnel, after passing an intermediate transfer matrix \tilde{M} , produces an exponentially decreasing function on the right-hand side. In the new basis, this property and the form eq. 5 require that the intermediate transfer matrix obeys $\tilde{M}_{22} = 0$.

3 Prop: In the system \tilde{M} of transfer matrices for finite strings, the condition for a bound state requires that the second diagonal element vanishes.

A tunnel of length b , followed by an attractive delta-potential of strength u at negative energy $E = -\frac{\hbar^2}{2m}\kappa^2$ we term the string S . We define $\delta := u/\kappa$ and $\lambda_1 := \exp(\beta)$, $\beta := \kappa b$ to obtain the transfer matrix of S as

$$\begin{aligned} \tilde{M}_1 &= \begin{bmatrix} (1 + \frac{1}{2}\delta) & \frac{1}{2}\delta \\ -\frac{1}{2}\delta & (1 - \frac{1}{2}\delta) \end{bmatrix} \begin{bmatrix} \lambda_1^{-1} & 0 \\ 0 & \lambda_1 \end{bmatrix} \\ &= \begin{bmatrix} \lambda_1^{-1}(1 + \frac{1}{2}\delta) & \lambda_1 \frac{1}{2}\delta \\ -\lambda_1^{-1} \frac{1}{2}\delta & \lambda_1(1 - \frac{1}{2}\delta) \end{bmatrix}. \end{aligned} \quad (7)$$

Here the first transfer matrix describes the delta-potential and the second one the tunnel, compare [12]. This and all other transfer matrices we take as a function of the dimensionless variable $\beta = \kappa b$, related to the energy and to the length of the cell S . We also consider them as a function of the variable $\gamma = ub$ related to the strength of the delta-potentials, and study the family of systems with varying strength. Instead of γ we shall often use the ratio $\delta := \frac{\gamma}{\beta}$ because then the matrix elements of \tilde{M}_1 are (linear) *polynomials in the variable* δ . Since we shall generate all other transfer matrices by matrix multiplication, a general transfer matrix will be a *polynomial in the parameter* δ . This will be the basis for a *polynomial method* for handling the analysis.

We introduce the following short-hand notation for the elements of a matrix \tilde{M}_i

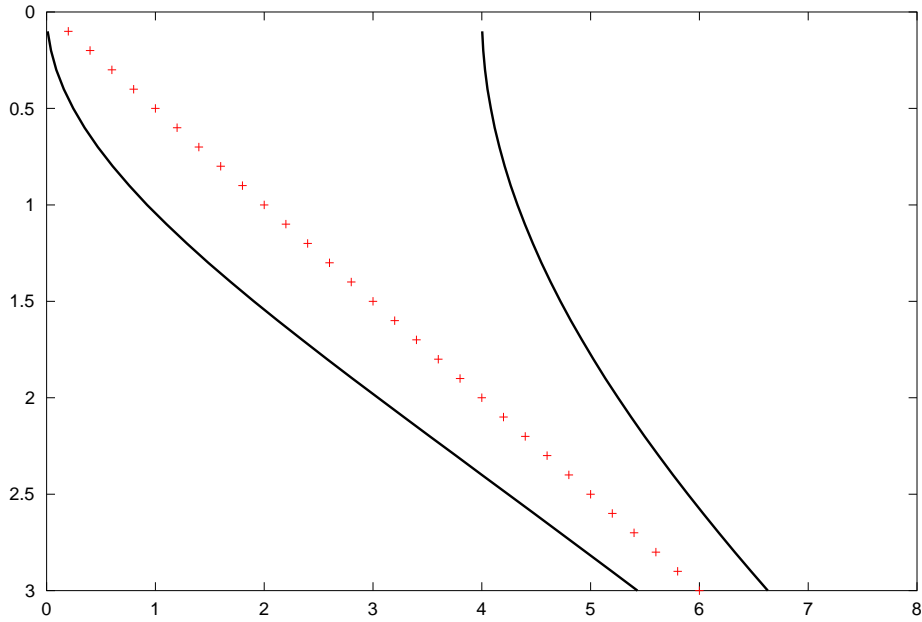
$$\tilde{M}_i := \begin{bmatrix} a_i & b_i \\ c_i & d_i \end{bmatrix} \quad (8)$$

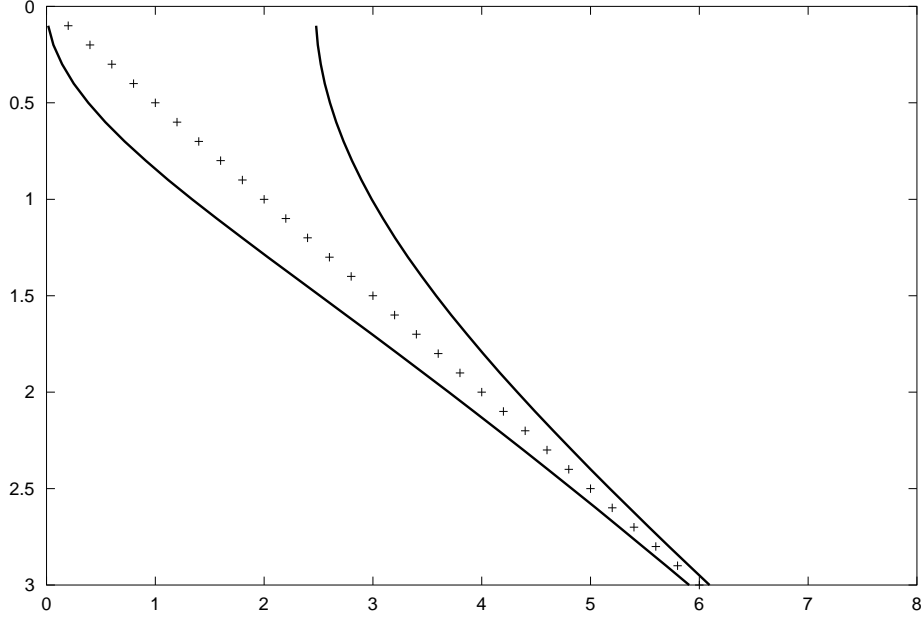
$$x_i := \frac{1}{2}(a_i + d_i),$$

$$y_i := \frac{1}{2}(a_i - d_i).$$

The second row of eq. 8 determines the *half-trace* $x_i = \frac{1}{2}tr(\tilde{M})$. For the matrix \tilde{M}_1 we find from eq. 7

$$\begin{aligned} x_1 &= \frac{1}{2}(\lambda_1 + \lambda_1^{-1}) - \frac{1}{4}\delta(\lambda_1 - \lambda_1^{-1}), \\ y_1 &= -\frac{1}{2}(\lambda_1 - \lambda_1^{-1}) + \frac{1}{4}\delta(\lambda_1 + \lambda_1^{-1}), \\ d_1 &= \lambda_1(1 - \frac{1}{2}\delta). \end{aligned} \tag{9}$$





Figs 2,3: The strings of length $\kappa b = 1, \tau$ respectively produces two different band germs which encapsulate the same bound state. Here and in all the corresponding Figures, the values of γ and β determine the potential strength and the energy respectively and are plotted as the horizontal and vertical coordinates respectively.

We shall assume that we are in the band germ and, moreover, that the upper edge of the band occurs at negative energy. In sections 4,5 we shall deal with more general scenarios. For $|x_1| \leq 1$, the eigenvalues of \tilde{M}_1 are complex conjugate of modulus 1 given by

$$\theta_1 = x_1 + i\sqrt{1 - x_1^2}, \quad \theta_2 = x_1 - i\sqrt{1 - x_1^2}. \quad (10)$$

So x_i is the half-trace, and the local Bloch label K for fixed energy is obtained from

$$\cos(Kb) = x_1(\beta, \gamma), \quad 0 \leq K \leq \frac{\pi}{b}. \quad (11)$$

The values $\beta : x_1(\beta) = -1, 1$ determine the two band edges respectively. The lower diagonal element by $d_1(\beta) = 0$ determines, compare [12] and what was explained above, the *single bound state of the delta-potential* at $\delta = \frac{u}{\kappa_0} = 2$. The variable λ_1 , related to the tunnel length, drops out of this equation.

As \tilde{M} is real, the eigenvectors can be chosen complex conjugate. We find

$$\tilde{M}_1 V = V \Lambda, \quad (12)$$

$$V = \begin{bmatrix} p & \bar{p} \\ v & \bar{v} \end{bmatrix}$$

$$\Lambda = \begin{bmatrix} \theta_1 & 0 \\ 0 & \theta_2 \end{bmatrix}.$$

with

$$\frac{v}{p} = \frac{\theta_1 - a_1}{b_1} = \frac{-y_1 + i\sqrt{1-x_1^2}}{b_1} \quad (13)$$

$$= \delta^{-1} \left[(1 - \lambda_1^{-2}) - \frac{1}{2}\delta(1 + \lambda_1^{-2}) + 2i\lambda_1^{-1}\sqrt{1-x_1^2} \right].$$

With the help of the matrix V we pass to the Bloch system of solutions defined by $M(x)\tilde{R}V$ since it obeys $M(0)\tilde{R}V = \tilde{R}V$, $M(b)\tilde{R}V = \tilde{R}V\Lambda$. In line with eq. 12 we mark derivatives with respect to x with a prime and put

$$M_1(x)\tilde{R}V := \begin{bmatrix} \Phi_1 & \Phi_2 \\ \Phi'_1 & \Phi'_2 \end{bmatrix}, \quad (14)$$

$$\Phi_2 = \bar{\Phi}_1,$$

and obtain for $0 < x < b$ from eqs. 12,13,14 the Bloch state

$$\Phi_1(x) := \frac{p}{\sqrt{2\kappa}} \left[\exp(-\kappa x) + \delta^{-1} \left[(1 - \lambda_1^{-2}) - \frac{1}{2}\delta(1 + \lambda_1^{-2}) + 2i\lambda_1^{-1}\sqrt{1-x_1^2} \right] \exp(\kappa x) \right]. \quad (15)$$

To normalize the current density to the value $\frac{e\hbar}{2m}$ it suffices to choose $\det(V) = p\bar{v} - v\bar{p} = -i$ which together with eq. 13 yields

$$p\bar{p} = \frac{\delta\lambda_1}{4\sqrt{1-x_1^2}}, \quad p = i\frac{1}{2}\sqrt{\frac{\delta\lambda_1}{\sqrt{1-x_1^2}}}, \quad (16)$$

where we have chosen a particular phase for p so that $\bar{p} = -p$. The two Bloch states obey the bilinear relation

$$(-i)(\bar{\Phi}_l\Phi'_j - \bar{\Phi}'_l\Phi_j) = (-1)^{l+1}\delta_{lj}. \quad (17)$$

which can be used to define a *scalar product* for Bloch states:

4Def: To any pair Φ_1, Φ_2 of complex solutions of the Schrödinger equation we can associate an indefinite hermitian scalar product $\langle \Phi_1, \Phi_2 \rangle$ by the left-hand side of eq. 17.

The relation between the Bloch states and the exponential states $M_1(x)\tilde{R}$ is given from eqs. 12 and 14 by

$$\begin{bmatrix} \psi_1 & \psi_2 \\ \psi'_1 & \psi'_2 \end{bmatrix} := M_1(x)\tilde{R} = (M_1(x)\tilde{R}V) V^{-1} \quad (18)$$

$$= \begin{bmatrix} \Phi_1 & \Phi_2 \\ \Phi'_1 & \Phi'_2 \end{bmatrix} i \begin{bmatrix} \bar{v} & -\bar{p} \\ -v & p \end{bmatrix}$$

A particular case arises if we choose the bound state energy $E = -\frac{\hbar^2}{2m}\kappa_0^2$ and construct the Bloch states eq. 14 for $\kappa = \kappa_0, \delta = 2$. This bound state must increase exponentially in the unit cell towards the delta-potential and is given from eqs. 15, 16 and 18 for $0 < x < b$ by

$$\psi_2(x) = -\frac{1}{2} \sqrt{\frac{2\lambda_1}{\sqrt{1-\lambda_1^{-2}}}} (\Phi_1(x) + \Phi_2(x)). \quad (19)$$

which differs from the expression given in [12] eq.(22) in the phase for the Bloch states and due to the new sequence of tunnel and potential. A natural real unbound companion of this bound state from eq. 18 is

$$\psi_1(x) = i(\Phi_1(x)\bar{v} - \Phi_2(x)v), \quad (20)$$

because it can be easily be shown that the scalar product eq. 17 for these two real states yields the Wronskian

$$\psi_1\psi_2' - \psi_1'\psi_2 = 1. \quad (21)$$

Here we wish to comment on the method of orthogonalized plane waves *OPW* in which Bloch states are required to be orthogonal to certain bound states [2] p.206-208. We doubt that this requirement can be handled with the standard integral scalar product in Hilbert space, or with a scalar product that involves only integration over the unit cell: The first integration does not apply without qualification to unbound states, and the second one introduces terms at the boundary of the unit cell.

2.3 The string S^n .

Now we pass from the string S by n-fold repetition to the string S^n with the transfer matrix \tilde{M}_1^n . This power of \tilde{M}_1 can be written as

$$\tilde{M}_1^n = V\Lambda^n V^{-1}. \quad (22)$$

Explicitly the four matrix elements from eqs. 12, 13, 14 are

$$\begin{aligned} a_n &= a(\tilde{M}_1^n) = \cos(nKb) + y_1 \frac{\sin(nKb)}{\sin(Kb)}, \\ d_n &= d(\tilde{M}_1^n) = \cos(nKb) - y_1 \frac{\sin(nKb)}{\sin(Kb)}, \\ b_n &= b(\tilde{M}_1^n) = \frac{1}{2}\lambda_1 \delta \frac{\sin(nKb)}{\sin(Kb)}, \\ c_n &= c(\tilde{M}_1^n) = -\frac{1}{2}\lambda_1^{-1} \delta \frac{\sin(nKb)}{\sin(Kb)}. \end{aligned} \quad (23)$$

with y_1 taken from \tilde{M}_1 in eq. 7.

2.4 Rational Bloch labels.

Consider the transfer matrix eqs. 22, 23 for the unit cell. For fixed integer $n > 0$ at the points

$$nKb = \mu\pi, \mu = 0, \pm 1, \dots, \pm(n-1), \pm n \quad (24)$$

it becomes $\tilde{M}_1^n = (-1)^n e$. For any such Bloch label it follows that the Bloch states have the period $2nb$ with symmetry group C_{2n} . We can relate these states to a chain of n atoms by imposing as boundary conditions the factor $(-1)^n = \pm 1$ for even and odd n respectively on the interval nb . Moreover the Bloch state for fixed μ on the unit cell transforms according to the representation

$$D^\mu = \exp(i\mu \frac{2\pi}{2n}) \quad (25)$$

for the generator of order $2n$ of the cyclic group C_{2n} .

There is *degeneracy* as we have a real hamiltonian: For opposite signs of Kb and μ we have pairs of Bloch states with equal energy, running to the left and right respectively. The set of rational states for fixed n yields a spectrum of (in part) conjugate eigenstates. The energy increases with $|\mu|$. The rational states are shown for $n = 2, 3$ in Figs. 5, 6.

With respect to C_{2n} , each eigenstate is characterized by a real or by a pair of complex conjugate irreducible representations of C_{2n} . All these rational states occur in the band and separate it into n partial bands characterized by

$$K \geq 0 : \frac{\mu\pi}{nb} \leq K \leq \frac{(\mu+1)\pi}{nb}, \mu = 0, 1, \dots, (n-1), n. \quad (26)$$

and similar expressions for $K \leq 0$.

2.5 Bound states and clusters of the string S^n .

The bound states of the finite string S^n are characterized from eq. 23 by

$$\begin{aligned} d(\tilde{M}_1^n) &= 0, \\ \tan(nKb) &= \frac{\sin(Kb)}{y_1}. \end{aligned} \quad (27)$$

The free string forms a cluster with n atoms and hence at most n bound states. We now compare these bound states with the states of the (up to a sign) periodic string of n atoms: In the interval between two successive zeros of $\tan(nKB)$ with $nKb = \mu\pi, (\mu+1)\pi$, which correspond to the rational K labels associated with states of the periodic string, the value of $\tan(nKb)$

goes once to infinity. The right-hand side of eq. 27 is a smooth function of β except at the point $y_1(\beta) = 0$. The left and right-hand side of eq. 27 are displayed for the case $n = 10$ as functions of β in Fig.4.

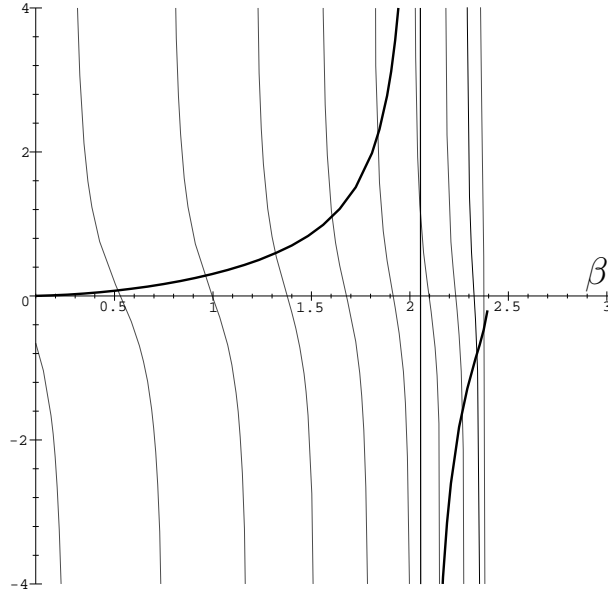


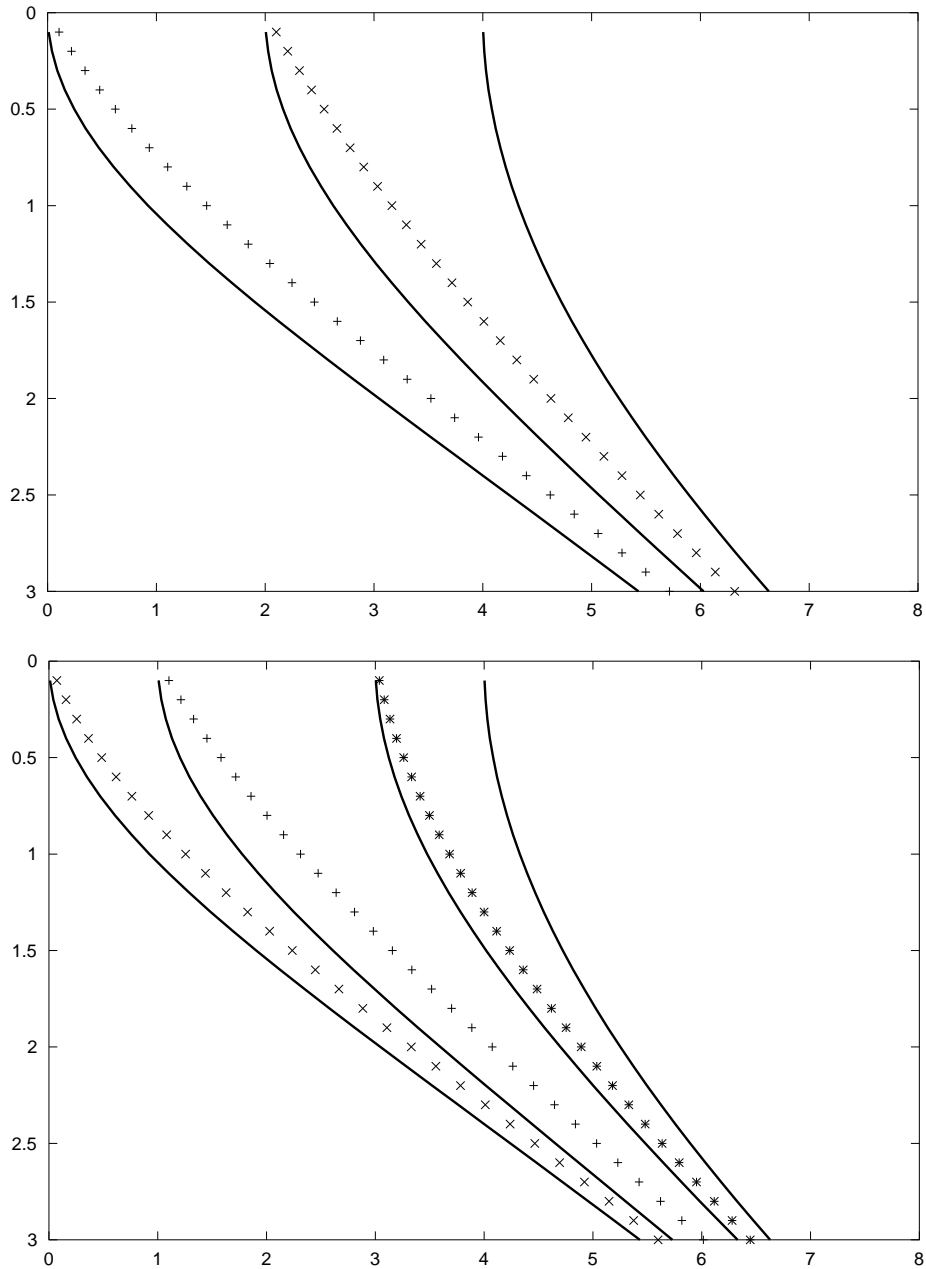
Fig.4: Left- and right-hand side of the binding eq. 27 on a string of length 10 for $\gamma = 4$ as a function of β .

On any interval between consecutive zeros of $\tan(nKb)$ there is precisely one intersection point of the left and the right-hand expression of eq. 27.

In terms of boundary conditions this implies that, in between the energies of two consecutive rational values of Kb with periodic boundary conditions, there is precisely one bound state of the n -atom cluster. This state, termed a *decaying state* in [12], is a single linear combination of two degenerate Bloch states on the interval of length nb and, when the n -atom string is cut out, admits exponential decay to the right and to the left.

5 Prop: Any set of rational Bloch labels eq. 24 separates the band into n partial bands. Each partial band contains a single bound state of the free n -atom string.

The relation between rational Bloch labels and bound states is shown in the following Figs. 5,6.



Figs. 5,6: The strings S^2 and S^3 . In the supercell analysis, two or three band germs are glued together without gaps and overlaps. Each band includes a single bound or decaying state. The horizontal coordinate is the potential strength γ , the vertical coordinate the energy β . Notice the relation between the onset of additional bound states and the subband edges.

Since the rational labels K form a dense set of energies, we must also have a dense set of bound or decaying state energies of free n -atom strings. Each

bound state coincides on a cell of length nb with a linear superposition of two Bloch states at the same fixed negative energy similar to ψ_2 in eq. 19. Each one has a companion state of a form similar to ψ_1 in eq. 20, and these two states have a Wronskian as in eq. 21.

2.6 Participation number.

From the relation between n -atom clusters and periodic states we can assign within a band a *participation number* n to the rational Bloch vectors of the form $K = \frac{\mu\pi}{nb}$, eq. 24: This number determines the number n of atoms which participate in the Bloch states whose period up to a sign is nb , and at the same time assigns n bound or decaying states of the cluster. Small values of n indicate states which involve a few atoms and may be called localized with respect to the clusters.

2.7 Supercell interpretation.

An alternative interpretation of the results given above can be given in terms of a *supercell scheme*: We consider the supercell of length nb formed from n centers. The corresponding Brillouin zones have the size $2\pi/(2bn)$. The positive Bloch labels for the n bands in this scheme are obtained from eq. 26 as

$$\begin{aligned} 0 \leq K(n, \mu) &= K - \frac{\mu\pi}{nb} \leq \frac{\pi}{nb}, \\ \mu &= 0, 1, \dots, (n-1), n \end{aligned} \quad (28)$$

and similar expressions for $K(n, \mu) \leq 0$. With the new Bloch label $K(n, \mu)$, these superbands are identical with the partial bands for the rational values of K .

6 Prop: The superbands for the supercell of length nb are glued together without gaps and overlaps and fill up the single band. Their Bloch states are identical to those of the partial bands of the rational scheme. Within each superband there is included a single bound state. This bound state coincides on the supercell with a bound state of the free n -atom cluster which forms the motive of the supercell. The alternating pattern of bound and periodic n -atom states illuminates the structure of the band.

2.8 Large n limit.

Now we consider the limit $n \rightarrow \infty$. The rational K -labels form a dense set on the Brillouin zone. The length of the periodic chains and of the

clusters increases with the participation number. As the rational numbers form a dense set on the Brillouin zone, we have pairs of Bloch states and bound states near any value of K in the band. By picking rational values of K characterized by n , we select a set of periodic states which pairwise encapsulate bound states of the finite string S^n .

From the equal spacing of the zeros of $\tan(nKb)$ with respect to the band label K , and from the inclusion property for bound states there follows

7 Prop: The density of bound and of Bloch states in the limit $n \rightarrow \infty$ is a constant function of the Bloch label K . In this limit, the density of (bound) states per unit energy interval fulfills the well-known relation

$$\frac{dN}{dE} \sim \frac{dK}{dE}. \quad (29)$$

Although this is a smooth function in the limit, its rational approximants with large but finite n may look quite irregular as functions of β .

3 Finite Quasiperiodic strings at negative energy.

As an example of a quasiperiodic system we shall take the well-known Fibonacci system: We maintain delta-potentials of equal strength for the atoms but admit two different intervals S and L of length b and qb respectively. For the proper Fibonacci case we choose $q = \tau = \frac{1}{2}(1 + \sqrt{5})$, but for comparison with the periodic case we also consider the value $q = 1$.

The Fibonacci system we define algebraically by the recursive words W_m and initial data in the alphabet $\langle S, L \rangle$,

$$W_{m+1} := W_{m-1}W_m, \quad W_1 = S, W_2 = L. \quad (30)$$

The word W_m contains f_m letters, f_{m-1} letters S , and f_m letters L . Here f_m are the integer Fibonacci numbers defined by $f_{m+1} = f_{m-1} + f_m$, $f_1 = f_2 = 1$.

3.1 Preview: Energy gauge in Fibonacci strings.

As an introduction we take from [12] the example of two strings S, L which represent the same attractive delta-potentials combined with tunnels of length b and τb respectively and then pass to the string SL . The energy gauges for S and L both contain the same bound state. The string SL has two bound states but may have, depending on the tunnel length, two or one band germ. In the first case there exists a region of negative energy where the single

strings admit band germs but the combined string SL does not. This case is schematically represented in Fig.7.

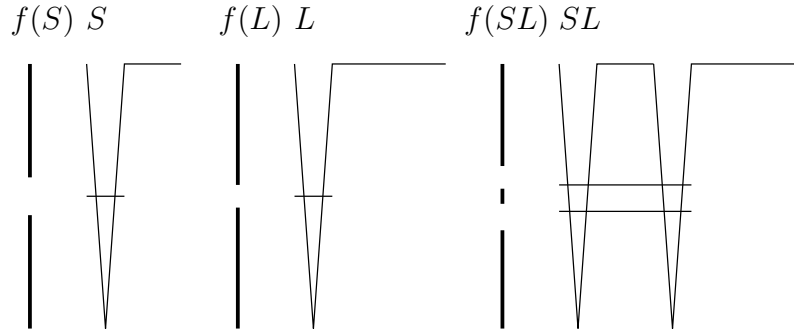


Fig.7: Fibonacci strings: The string S to the left and its energy gauge $f(S)$ are as in Fig. 1. The string L in the middle has the same bound state within the gauge $f(L)$ of smaller width. The string SL to the right has two attractive δ -potentials and hence the same bound states as S^2 in Fig. 1. In contrast to S^2 , the string SL has two separate band germs. The corresponding two parts of the energy gauge $f(SL)$ comprise each one bound state but block the energy of the single-atom bound state.

3.2 Substitutional systems and their invariants.

The Fibonacci system to be considered can be seen as a particular case of a substitutional system. We shall restrict our attention to substitutional systems generated by automorphisms of the free group. For these algebraic concepts in general we refer to [13] and follow in detail [10]. Consider the free group F_2 with generators (alphabet) a_1, a_2 . Its elements are all the words in the generators and their inverses. An automorphism of F_2 is defined as a map

$$\rho : a_1, a_2 \rightarrow f_1(a_1, a_2), f_2(a_1, a_2) \quad (31)$$

which is *algebraically invertible* so that a_1, a_2 can be expressed in terms of f_1, f_2 .

Example: Consider the substitution $a_1, a_2 \rightarrow f_1 = a_2, f_2 = a_1 a_2$. Its inverse is given by $a_1 = f_2 f_1^{-1}, a_2 = f_1$. This substitution describes in abstract terms the Fibonacci systems to be discussed below.

For any automorphism of F_2 we have the general theorem

8 Prop (Nielsen 1918): For ρ an automorphism of F_2 , the commutator $\mathcal{K}(a_1, a_2) := a_1 a_2 a_1^{-1} a_2^{-1}$ obeys

$$\rho(\mathcal{K}) = w \mathcal{K}^{\pm 1} w^{-1} \quad (32)$$

with $w \in F_2$.

Example: For the Fibonacci automorphism one finds

$$\rho(\mathcal{K}) = \mathcal{K}^{-1} \quad (33)$$

From this abstract algebraic set-up we can pass to matrix systems by first mapping the generators a_1, a_2 to two elements of a matrix group like $SL(2, R)$ for the transfer matrices and then performing the automorphism ρ induced on the matrix group. For certain classes of such induced automorphisms, one can obtain the (half-) traces of the images directly from the (half-) traces of the generators. This question is studied in the theory of *trace maps* for which we refer to Peyrière [16]. The Fibonacci automorphism and related systems belong to this class [10]. The Nielsen theorem in connection with the induced automorphisms now provides one or more *invariants of induced automorphisms*: Consider the induced commutator \mathcal{K} on the matrix group $SL(2, R)$ and take its trace. Under the Fibonacci automorphism the commutator as a matrix is transformed into its inverse. Since all matrices are unimodular, we get on the matrix group

$$tr(\rho(\mathcal{K})) = tr(\mathcal{K}^{-1}) = tr(\mathcal{K}) \quad (34)$$

9 Prop: The trace of the commutator is an invariant under the Fibonacci substitution.

The commutator $K(g_1, g_2)$ in a matrix group is a measure of the non-commutativity. In particular if the two matrices commute, the half-trace eq. 34 must be 1. Conversely if \mathcal{K} equals the unit matrix, the elements g_1, g_2 commute. We shall come back to this property in later sections.

3.3 Recursive calculation of the transfer matrix.

To represent the Fibonacci system by delta-potentials and the states by transfer matrices we define

$$\tilde{M}(S) := \tilde{M}_1, \quad \tilde{M}(L) := \tilde{M}_2. \quad (35)$$

We represent the Fibonacci string W_{m+1} of eq. 30 by the transfer matrix

$$\tilde{M}_{m+1} = \tilde{M}_{m-1} \tilde{M}_m. \quad (36)$$

The transfer matrix \tilde{M}_2 has the same analytic form as \tilde{M}_1 given in eq. 7 with the same variable δ and the same energy E but with the replacement

$$\lambda_1 = \exp(\beta) \rightarrow \lambda_2 := \exp(q\beta). \quad (37)$$

Similar systems have been studied extensively in the literature, compare references given by Kohmoto [9] and in [3]. Many of these studies used a discrete version or examined the recursion numerically. In what follows we shall use the recursive method to explore the *analytic structure* of the Fibonacci strings as functions of the variables β, δ . We recall that \tilde{M}_1, \tilde{M}_2 eqs. 7, 35 are linear polynomials with respect to δ . From this property and from eq. 36 we get immediately :

10 Prop: The matrix elements of \tilde{M}_m are polynomials of degree f_m with respect to the parameter δ , with coefficients which are functions of β via the expressions λ_1, λ_2 .

For the finite Fibonacci string we wish to study the matrix elements of the transfer matrix \tilde{M}_i and in particular their combinations $x_i, y_i, d_i = (x_i - y_i)$, since they yield information on the eigenvalues and bound states. Two methods are available for the computation:

(i) We can use the full matrix recursion eq. 36, with the starting matrices \tilde{M}_1, \tilde{M}_2 .

(ii) We can use recursion techniques for the half-traces and the other matrix elements, as was proposed in [10]. From this reference we deduce the following recursion equations for the combinations of matrix elements:

$$\begin{aligned} \begin{bmatrix} a_{m+1} & b_{m+1} \\ c_{m+1} & d_{m+1} \end{bmatrix} &= \begin{bmatrix} a_m + d_m & 0 \\ 0 & a_m + d_m \end{bmatrix} \begin{bmatrix} a_{m-1} & b_{m-1} \\ c_{m-1} & d_{m-1} \end{bmatrix} \\ &- \begin{bmatrix} d_{m-2} & -b_{m-2} \\ -c_{m-2} & a_{m-2} \end{bmatrix}, \\ x_{m+1} &= 2x_m x_{m-1} - x_{m-2}, \\ y_{m+1} &= 2x_m y_{m-1} + y_{m-2}, \\ d_{m+1} &= x_{m+1} - y_{m+1}. \end{aligned} \quad (38)$$

To start these recursive relations we need the matrices \tilde{M}_1, \tilde{M}_2 given from eqs. 7, 35 and compute \tilde{M}_3 from

$$\begin{aligned} \tilde{M}_3 &= \tilde{M}_1 \tilde{M}_2 : \\ a_3 &= \lambda_1^{-1} \lambda_2^{-1} (1 + \frac{1}{2} \delta)^2 - \frac{1}{4} \lambda_1 \lambda_2^{-1} \delta^2, \\ b_3 &= \frac{1}{2} \lambda_1^{-1} \lambda_2 \delta (1 + \frac{1}{2} \delta) + \frac{1}{2} \lambda_1 \lambda_2^{-1} \delta (1 - \frac{1}{2} \delta) \\ c_3 &= -\frac{1}{2} \lambda_1^{-1} \lambda_2^{-1} \delta (1 + \frac{1}{2} \delta) - \frac{1}{2} \lambda_1 \lambda_2^{-1} \delta (1 - \frac{1}{2} \delta) \\ d_3 &= \lambda_1 \lambda_2 (1 - \frac{1}{2} \delta)^2 - \frac{1}{4} \lambda_1^{-1} \lambda_2 \delta^2. \end{aligned} \quad (39)$$

These matrix elements are polynomials of degree 2 in the variable δ as expected. The half-traces x_m form a recursive system by themselves. This is the well-known *Fibonacci trace map*.

11 Prop: By use of the recursive relations eq. 38 we can construct algebraic polynomial expressions of degree f_m for the half-trace $x_m(\beta, \delta)$ and for the matrix element $d_m(\beta, \delta)$, which we call the *band polynomial* and the *bound polynomial* respectively. The edges of the band germs for the Fibonacci string W_m are given by the f_m roots of the *band polynomial equations*

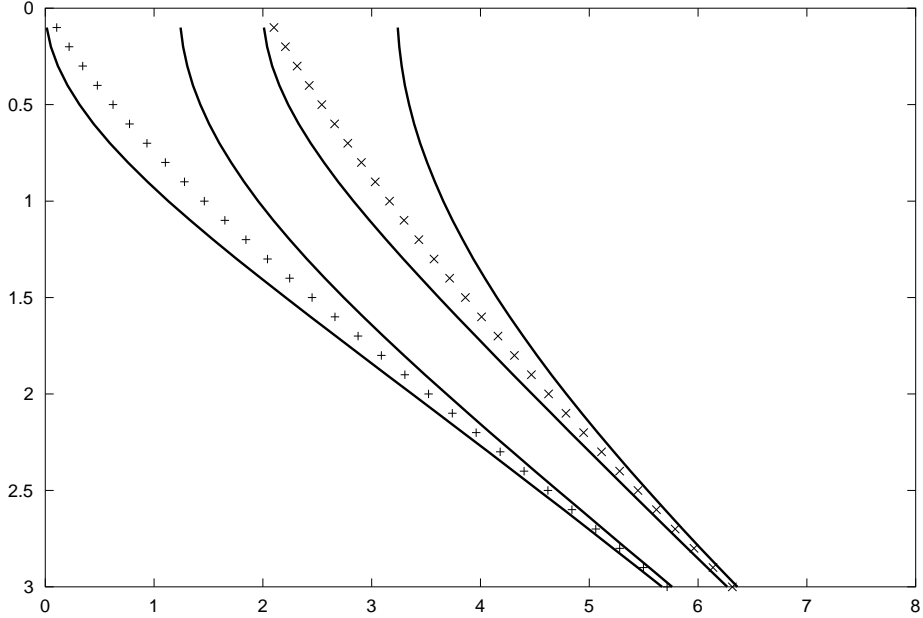
$$x_m(\beta, \delta) = \pm 1, \quad (40)$$

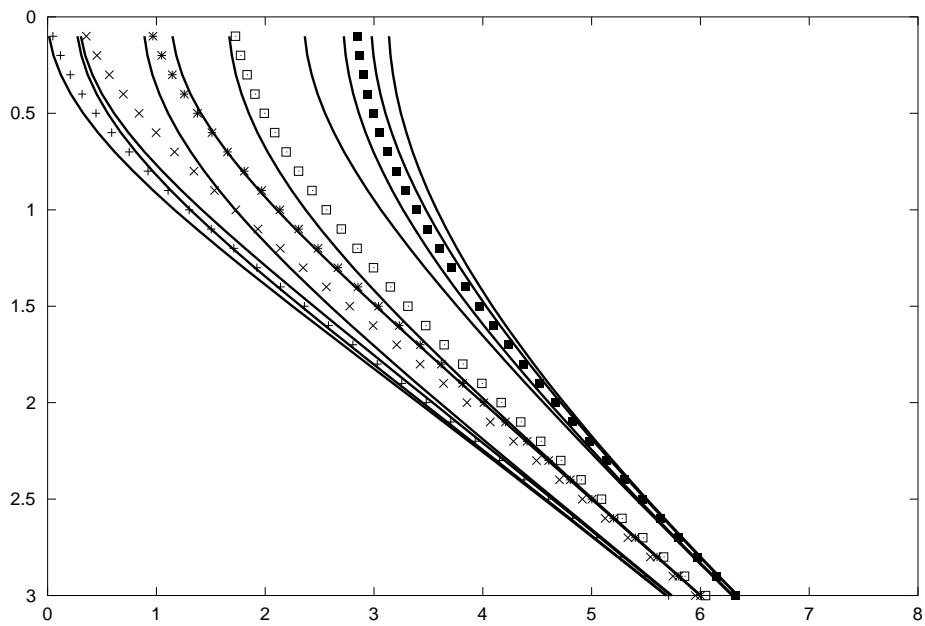
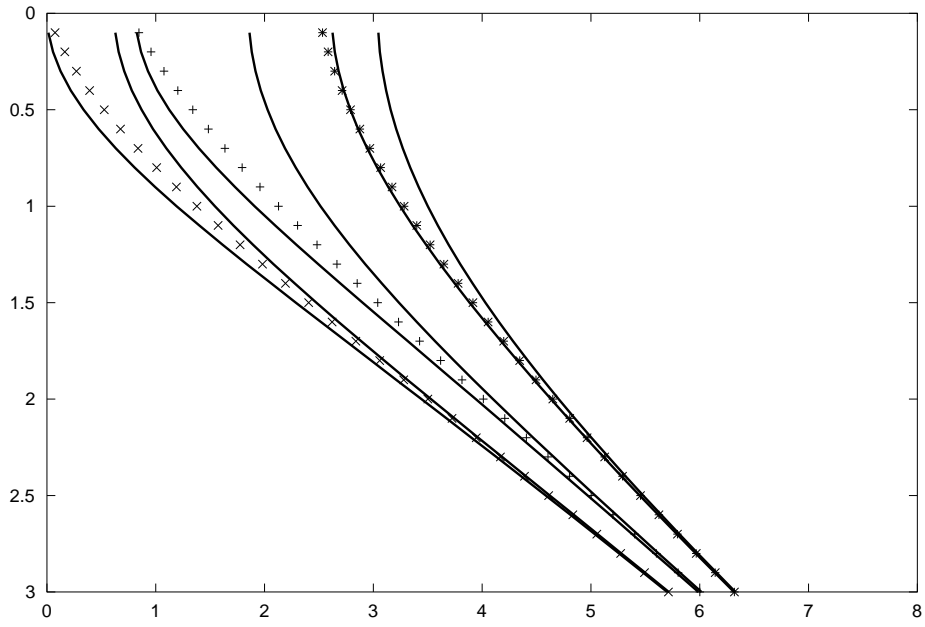
while the bound states are given as the f_m roots of the *bound polynomial equations*

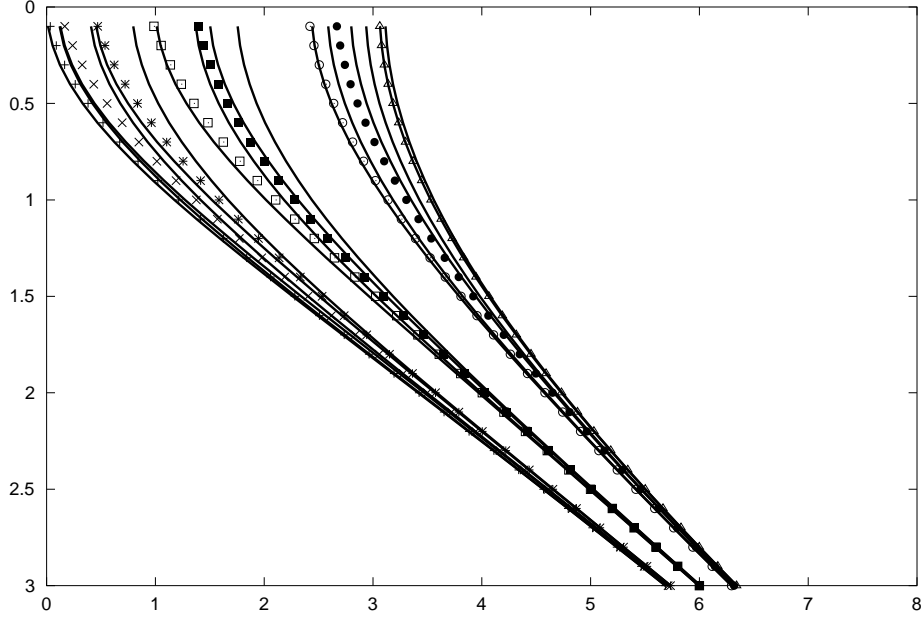
$$d_m(\beta, \delta) = 0. \quad (41)$$

The f_m roots of the polynomials eq. 40 are real since they represent special half-traces of real matrices. The f_m roots of the polynomial eq. 41 are real for sufficient strength of the delta-potential since then we must get f_m bound states.

For low values of m the roots of the polynomials can be obtained in closed algebraic form.







Figs 8-11: Band germs and bound or decaying states as functions of γ horizontal and β vertical for Fibonacci strings of 3-6 atoms. The bound states are not always inside the band germs. The band germs which were glued in the periodic string are now all separated. The number of band germs increases proportional to the number of atoms.

In Figs. 8-11 we use the roots of eqs. 40, 41 to plot for the first 6 Fibonacci strings the edges of band germs and the bound states as functions of β , negative vertical coordinate, and γ , horizontal coordinate. For each value of m , we compare the periodic case $q = 1$ with the quasiperiodic case $q = \tau$. For the value $q = 1$ we are back at periodic cases and would obtain glued systems of 2, 3, 5, 8 superbands respectively in a way similar to Figs. 5, 6. These superbands encapsulate the bound states of the free clusters. For the Fibonacci case $q = \tau$ there appears a system of f_m band germs, for any value of γ separated by gaps. The bound states for higher values of γ are encapsulated within these band germs. For large fixed values of γ the band germs become narrow and form a triple of subsets. The latter feature may be related to the occurrence of isolated 2-atom clusters at the short distance b in the Fibonacci strings. These may be considered as examples of motive clusters discussed in section 1. The locally symmetric or antisymmetric hybrid states of these clusters can be related to the lowest and highest subset. Figs. 8-11 also demonstrate how the quasiperiodic system develops under the Fibonacci recursion or inflation. If one looks for fixed strength γ at the interchange of bands and gaps, one observes a permanent change of the density of states (DOS). In an approximant computation of this quasicrystal

one would stop at a certain length and obtain the DOS from the band germ analysis of the corresponding string. In view of the present examples it is hard to believe that this method describes the real DOS of the quasicrystal.

In a periodic potential we get a finite number of bands at least at negative energy which can encompass a number of electron states proportional to the number of atoms. In the Fibonacci strings notice that, in marked contrast to the periodic case, when extending the Fibonacci string the number of band germs which encapsulate bound states *increases proportional to the number of delta-potentials*, i.e. *proportional to the number n of atoms*, each with one electron, in the model. If this is so, then the DOS cannot be computed from the gap and band germ structure of the string. As we have only n electrons, it makes no sense to distribute them into a system of n bands. We conclude that in approximant computations of the DOS one should keep track of the number of bands in relation to the system size. Otherwise the conclusions on the DOS in the proper quasiperiodic system are doubtful.

Now we turn to the significance of the conserved quantity related to the trace of the commutator. This trace is related to the invariant I considered in [9] and [3] by

$$\frac{1}{2}tr(\mathcal{K}) = 2I + 1. \quad (42)$$

If the commutator becomes the 2×2 unit matrix we get $I = 0$. In [12] we computed the commutator for the present Fibonacci system with the result

$$\frac{1}{2}tr(\mathcal{K}) = 1 + \frac{1}{2}\left(\frac{u}{\kappa}\right)^2(\sinh(\kappa(\tau - 1)b)^2 \quad (43)$$

This expression is always larger than 1. It implies that *in the negative energy tight binding scenario the two transfer matrices never commute*. A different result will appear for positive energy and scattering.

4 Periodic strings at positive energy.

We turn to electron states at positive energy. To this end we use the analytic continuation from the variable κ to the variable k defined by

$$\kappa \rightarrow -ik. \quad (44)$$

For the energy we have now $E = \frac{\hbar^2}{2m}k^2 \geq 0$. For the variables β, δ we shall use

$$\beta \rightarrow -i\beta, \quad \delta \rightarrow i\delta. \quad (45)$$

So we maintain the symbol β as a real variable in what follows. We shall plot the positive energy range $E = \frac{\hbar^2}{2mb^2}\beta^2$ at negative values of the new real parameter β . Inserting the analytic continuation into the transfer matrix \tilde{M}_1 eq. 7 we find

$$\begin{aligned} x_1 &= \cos(\beta) - \frac{1}{2}\delta \sin(\beta), \\ y_1 &= i \sin(\beta) + i\frac{1}{2}\delta \cos(\beta), \\ \lambda_1 &= \exp(-i\beta) = \exp(-ikb). \end{aligned} \tag{46}$$

Similar expressions apply for \tilde{M}_2 .

4.1 The \mathcal{S} -matrix.

The transfer matrix of a finite string can be rationally related to the scattering matrix \mathcal{S} . For this purpose we shall use the transfer matrix in a form similar to eq. 5 which corresponds to exponential functions. The analytic continuation eqs. 44,45 is made both in $M(x)$ and with the matrix $R := \frac{1}{\sqrt{i}}\tilde{R}$ used instead of \tilde{R} . We redefine for positive energy

$$\tilde{M}(x) := R^{-1}M(x)R. \tag{47}$$

The negative energy tunnels with \tilde{M} given by eq. 6 become positive energy channels. The new fundamental system of solutions is

$$M(x)R = \sqrt{\frac{1}{2k}} \begin{bmatrix} \exp(ikx) & \exp(-ikx) \\ ik \exp(ikx) & -ik \exp(-ikx) \end{bmatrix}. \tag{48}$$

and consists of free plane waves running to the left and right respectively. The transfer matrix in the channels becomes

$$\begin{aligned} \tilde{M}(x) &:= R^{-1}M(x)R \\ &= \begin{bmatrix} \exp(ikx) & 0 \\ 0 & \exp(-ikx) \end{bmatrix}. \end{aligned} \tag{49}$$

Consider now a finite string of length h with transfer matrix \tilde{M} and with free channels on the left and right respectively. Denote the amplitudes on the left and right of the string by l_+, l_- and r_+, r_- respectively. These amplitudes are related by

$$\begin{bmatrix} r_+ \\ r_- \end{bmatrix} = \begin{bmatrix} a & b \\ c & d \end{bmatrix} \begin{bmatrix} l_+ \\ l_- \end{bmatrix}. \tag{50}$$

The elements of the scattering matrix are now determined by the ratio of amplitudes under certain boundary conditions and by phase factors which account for the length h of the string. For *scattering from the left* we obtain

$$\begin{aligned}
r_- &= cl_+ + dl_- = 0, \\
S_{++} &= \frac{r_+}{l_+} \exp(-ikh) \\
&= d^{-1} \exp(-ikh), \\
S_{-+} &= \frac{l_-}{l_+} \\
&= -d^{-1}c.
\end{aligned} \tag{51}$$

For *scattering from the right* we get

$$\begin{aligned}
l_+ &= dr_+ - br_- = 0, \\
S_{--} &= \frac{l_-}{r_-} \exp(-ikh) \\
&= -d^{-1} \exp(-ikh), \\
S_{+-} &= \frac{r_+}{r_-} \exp(-2ikh) \\
&= -d^{-1}b \exp(-2ikh).
\end{aligned} \tag{52}$$

Here S_{++} and S_{-+} are the amplitudes of *forward* and of *backward scattering* respectively. These expressions are given and discussed in [10] eqs.(50-54).

12 Prop: The scattering matrix \mathcal{S} has elements which are rational expressions in the transfer matrix \tilde{M} . The full scattering matrix becomes

$$\begin{aligned}
\mathcal{S} &:= \begin{bmatrix} S_{++} & S_{+-} \\ S_{-+} & S_{--} \end{bmatrix} \\
&= \begin{bmatrix} d^{-1} \exp(-ikh) & d^{-1}b \exp(-2ikh) \\ -d^{-1}c & d^{-1} \exp(-ikh) \end{bmatrix}.
\end{aligned} \tag{53}$$

The exponential factors arise by requiring that for the free transfer matrix on the string of length h we must have $\mathcal{S} = 1$. The expression for the \mathcal{S} -matrix in terms of the transfer matrix is non-linear but rational. We must compute \mathcal{S} from the transfer matrix of the full string, or otherwise evaluate all the backscattering effects from the components of the string. The unitarity of the \mathcal{S} -matrix and its transformation under time reversal follow from properties of the transfer matrix [10].

Consider now the analytic continuation eq. 44 in the inverse form

$$k \rightarrow i\kappa, \kappa \geq 0. \quad (54)$$

From inspection of eq. 53 under this analytic continuation we find

13 Prop: The poles of the scattering matrix eq. 53 on the positive imaginary k -axis are given by $d(\kappa) = 0$. These poles determine the bound states of the system, fully in line with the analysis given in eq. 41.

4.2 The \mathcal{S} -matrix for the periodic string S^n .

Again we consider a range of positive energy such that $|x_1| \leq 1$. This range may be called a band germ although it cannot correspond to bound states of the system. In this range we can find the eigenvalues and eigenstates of \tilde{M}_1 by analytic continuation of the expressions eqs. 8, 9. For the periodic string S^n with the transfer matrix \tilde{M}_1^n we find the same expressions as in eq. 23, but with y_1 and λ_1 now taken from \tilde{M}_1 in eq. 46. We shall again introduce a band label K by

$$\cos(Kb) = x_1 = \cos(\beta) - \frac{1}{2}\delta \sin(\beta). \quad (55)$$

Consider first the backward scattering determined from eq. 53 by c_n and d_n . The matrix element c_n oscillates rapidly with large n . We obtain *maximum backscattering* at the discrete values of the K -label

$$\begin{aligned} Kb &= \mu\pi, \mu = 0, \pm 1, \\ c_n &= -i\frac{1}{2}\lambda_1^{-1}(-1)^{\mu(n-1)}n\delta, \\ d_n &= (-1)^{\mu n}(1 - ny_1(-1)^\mu), \\ \exp(-ikh) &= \exp(-inkb). \end{aligned} \quad (56)$$

From

$$\cos(\mu\pi) = (-1)^\mu, \quad (57)$$

these maxima correspond to the *edges of the positive energy band germs* and become sharper with increasing n .

A *high-energy limit* is obtained for $\beta = kb \gg 1$. With $\delta = \gamma/\beta$, eq. 55 enforces

$$\beta = kb = Kb + \nu 2\pi + \epsilon. \quad (58)$$

Together with eq. 56, this equation yields *discrete values of k on the points of the reciprocal lattice*.

14 Prop: For large n and sufficiently high energy, the backscattering amplitude takes its non-vanishing values on the points of the reciprocal lattice. To lowest order in ϵ we find

$$\begin{aligned} x_1 &= (-1)^\mu, \\ y_1 &= i(-1)^\mu \frac{1}{2}\delta, \\ d_n &= (-1)^{\mu n} \left(1 - i\frac{1}{2}n\delta\right). \end{aligned} \tag{59}$$

In the high-energy limit we then get from eq. 53 at the band edges

$$\begin{aligned} S_{++} &= \frac{1}{1 - i\frac{1}{2}n\delta}, \\ S_{-+} &= \frac{i\frac{1}{2}n\delta}{1 - i\frac{1}{2}n\delta}. \end{aligned} \tag{60}$$

The limits $n \rightarrow \infty$ and of large energy should be distinguished from one another. In the limit $n \rightarrow \infty$ the absolute value of the backward scattering amplitude approaches its maximum $|S_{-+}| = 1$ allowed by unitarity, while the forward scattering amplitude goes to zero.

5 Quasiperiodic strings at positive energy.

The analytic continuation of the transfer matrix works for the Fibonacci strings. We simply must start the string with the analytic continuation of the starting matrices \tilde{M}_1, \tilde{M}_2 as given for \tilde{M}_1 in eq.46. Then we can apply the recursion technique of eq. 38 to find an algebraic expression for the transfer matrix of the Fibonacci string W_m .

5.1 The Fibonacci-atlas.

In principle we can construct the elements of the transfer matrix as polynomials of degree f_m with respect to δ for any order m . We obtain the corresponding \mathcal{S} -matrix from the relations eq. 53. In general it will be hard to obtain in this way closed limiting expressions as was possible in the periodic case. Nevertheless there are particular regions where closed expressions can be derived. We illustrate these regions in Fig.12 by plotting the band germs of both transfer matrices \tilde{M}_1, \tilde{M}_2 for $q = \tau$ as functions of the variables β, γ in the range $\beta \geq 0, \gamma > 0, \gamma < 0$. This plot we call the *Fibonacci-atlas*.

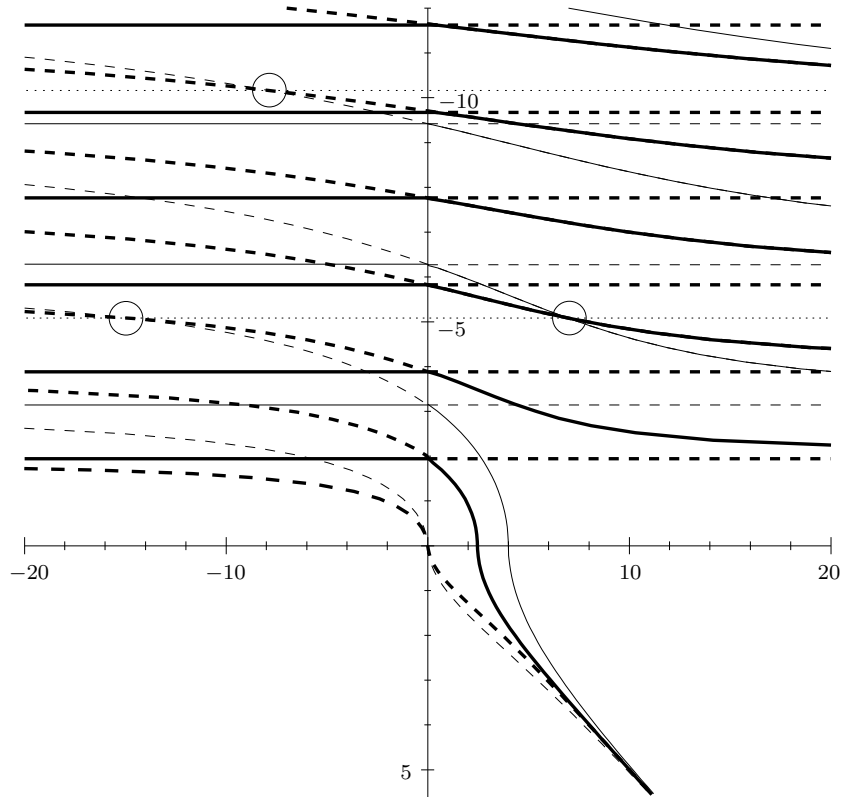


Fig.12: Fibonacci atlas: Band germs of the transfer matrices \tilde{M}_1, \tilde{M}_2 for positive and negative energy as functions of the energy variable β and the strength variable γ . Upper band edges drawn as full lines, lower band edges as dashed lines, heavy lines for the matrix \tilde{M}_2 . The two weak horizontal dotted lines mark values $\beta(p)$ where the two transfer matrices commute and give rise to extended states.

Consider again the commutator \mathcal{K} of the two transfer matrices. We must insert the analytic continuation to positive energy and obtain from eq. 43

$$\frac{1}{2}tr(K) = 1 + \frac{1}{2}\left(\frac{u}{k}\right)^2(\sin(k(\tau - 1)b))^2 \quad (61)$$

This expressions shows that there are periodic points where the half-trace becomes 1 and the invariant becomes $I = 0$. These points are given by

$$\beta(p) = \tau p \pi, \quad p = 0, 1, \dots \quad (62)$$

Moreover it was shown in [3] that the deviations $I - 1$ at these points starts quadratically with $(\beta - \beta(p))$. The values $\beta(p)$ are marked by dotted horizontal lines in Fig.12. If a line of this type intersects, depending on γ , with overlapping band germs for both transfer matrices, we obtain from $\lambda_2 = (-1)^p \lambda_1$

their proportionality,

$$\tilde{M}_2 = (-1)^p \tilde{M}_1. \quad (63)$$

15 Prop: At the values eq. 61, the two transfer matrices \tilde{M}_1, \tilde{M}_2 commute and are even proportional to one another.

More precisely we require three conditions at these special points: The half-traces of both transfer matrices should be smaller than 1, and the commutator should become the unit matrix. These conditions are controlled by the Fibonacci atlas Fig. 12: Consider a dotted horizontal line corresponding to commuting transfer matrices. For not too large values of γ , it runs inside overlaps of the two band germs which imply that both $|x_1| \leq 1, |x_2| \leq 1$. Outside this region, that is outside the points marked by circles in Fig. 12, we still have commuting transfer matrices, but their individual half-traces are larger than 1. It follows from algebraic properties of the group $SU(1,1)$ given in [10] that a vanishing commutator implies group elements of the same class type.

We can now see the advantage of the present algebraic and polynomial approach compared to numerical studies of the trace systems: For example in [3] the points eq. 62 were explored numerically and for fixed values of a strength $\gamma < 0$, corresponding to repulsive delta-potentials. The Fibonacci-atlas of Fig.12 now yields from closed algebraic expressions a full view on the regions of commutativity for all positive and negative values of γ and positive energy.

In a neighbourhood of such a commutative point we get, using the commutativity, for the full Fibonacci string W_m the transfer matrix

$$\tilde{M}_m = (-1)^{pf_{m-1}} \tilde{M}_1^{f_m}. \quad (64)$$

This transfer matrix agrees up to a factor with the transfer matrix of a periodic string of f_m delta-potentials with the spacing b . It follows that the \mathcal{S} -matrix of the Fibonacci strings near these points has the form and limiting values discussed in section 4.2.

16 Prop: In the neighbourhood of the discrete positive energies corresponding to eq. 62, the transfer and \mathcal{S} -matrix of the Fibonacci system are equivalent to those of a periodic string of length $f_m b$.

Some care is required because $\beta(p)$ in eq. 62 is not rational whereas for the periodic case we used the discrete labels Kb and $\beta = kb$. Note however that the value $\beta(p)$ for $p = f_l$ and not too small values of l is well approximated by the integral multiple $\beta = f_{l+1}\pi$ of π .

Finally in Fig. 13 we give the real wave function of an electron travelling at positive energy through a Fibonacci string of attractive delta potentials. The energy is tuned to a commutative value. At each passage through a delta potential, the derivative of the wave function jumps by a finite value.

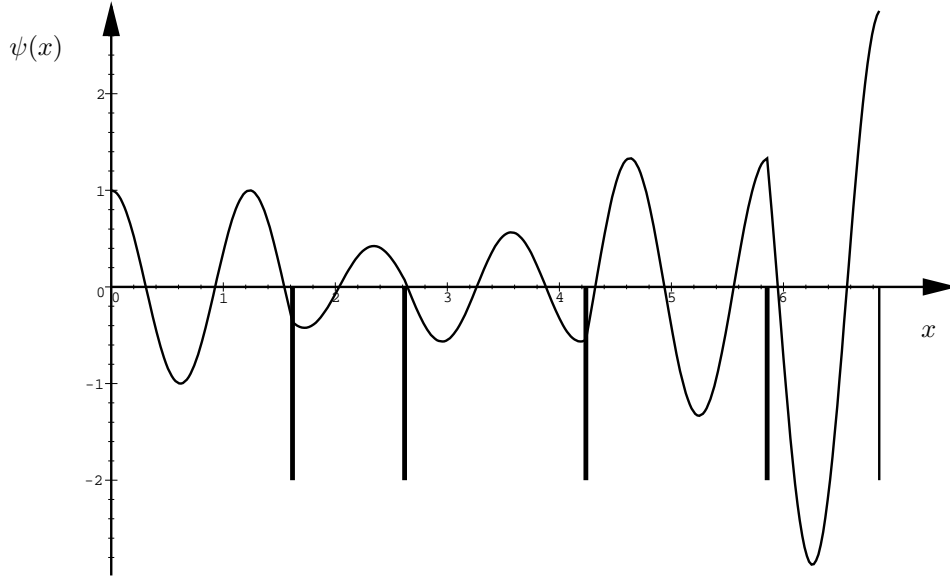


Fig. 13: Electron state propagating through a Fibonacci string of attractive delta-potentials at a positive energy where the transfer matrices commute.

6 Conclusion.

Our study of a very simple $1D$ electron system has demonstrated most of the points stated in general terms in the introduction, section 1. The local boundary conditions were implemented and related. The negative and positive energy scenarios showed different behaviour. At negative energy, the bound states have a clear relation to the Bloch states. In going from periodic to quasiperiodic strings, the glued and gap-less systems of superbands open gaps and split into subbands which encapsulate bound states. Motive clusters appear in the bound state energy. With increasing length of the Fibonacci string, the subband structure changes in a non-trivial fashion, with a number of subbands proportional to the number of atoms, and so puts question marks to approximant calculations. At positive energy, the band edges in periodic strings are related to maxima of scattering amplitudes. For quasiperiodic Fibonacci strings we gave closed algebraic expressions. At positive energies related by a period wrt. k , the transfer matrices commute and give rise to maxima in the scattering amplitudes.

References

- [1] Andersen O K, Jepsen O, Sob M, *Linearized Band Structure Methods*, Springer Lecture Notes, ed. M. Yussouff, Springer, Berlin (1987)
- [2] Ashcroft N W and Mermin N D, *Solid State Physics*, Saunders College, Philadelphia (1976)
- [3] Baake M, Joseph D and Kramer P, Phys. Lett. **A168** (1992) 199-208
- [4] Blount E I, *Formalism of Band Theory*, in: *Solid State Physics* **13**, eds. F. Seitz and D. Turnbull, Academic Press, New York (1962), 305-373
- [5] Cycon H L, Froese R G, Kirsch W, and Simon B, *Schrödinger Operators*, Springer, Berlin (1987), 197-216
- [6] Haerle R and Kramer P, Phys. Rev **B** (1998) in press
- [7] Heine V, *Electronic Structure from the Point of View of the Local Environment*, in: *Solid State Physics*, **35**, eds. F. Seitz and D. Turnbull, Academic Press, New York (1980), 1-127
- [8] Kohn W, Phys. Rev. **115** (1959) 332-344
- [9] Kohmoto M, Int. J. Mod. Phys. **B1** (1987) 31-49
- [10] Kramer P, J. Phys. **A26** (1993) 213-228
- [11] Kramer P, J. Phys. **A26** (1993) L245-L250
- [12] Kramer P, J. Phys. **A31** (1998) 743-756
- [13] Kramer P and Garcia-Escudero J, *Non-commutative Models for Quasicrystals*, in: *Beyond Quasicrystals*, eds. F. Axel and D. Gratias, Springer and Les Editions de Physique, Berlin and Les Ulis (1995), 55-73
- [14] Kramer P, Quandt A, Schlottmann M, and Schneider T, Phys. Rev. **B51** (1995) 8815-8829
- [15] Lieb E H and Mattis D C, *Mathematical Physics in One Dimension*, Academic Press, New York (1966)
- [16] Peyrière J, *Trace maps*, in: *Beyond Quasicrystals*, eds. F. Axel and D. Gratias, Springer and Les Editions de Physique, Berlin and Les Ulis (1995), 465-480
- [17] Skriver H L, *The LMTO Method: Muffin-Tin Orbitals and Electronic Structure*, Springer Series in Solid State Physics, Berlin (1984)

- [18] Sütö A, *Schrödinger difference equation with deterministic ergodic potentials*, in: *Beyond Quasicrystals*, eds. F. Axel and D. Gratias, Springer and Les Editions de Physique, Berlin and Les Ulis (1995), 483-549
- [19] Takeuchi S and Fujiwara T, *Proc. 6th Int. Conf. on Quasicrystals*, World Scientific, Singapore (1998)
- [20] Wannier G H, *Rev. Mod. Phys.* **34** (1962), 645-655
- [21] Wigner E P and Seitz F, *Phys. Rev.* **43** (1933), 804-810 and **46** (1934), 509-524